農研機構
NARO 国立研究開発法人 農業・食品産業技術総合研究機構

In situ characterization of acidic and thermal protein denaturation by infrared microspectroscopy

メタデータ	言語: eng 出版者: 公開日: 2019-05-14 キーワード (Ja): キーワード (En): 作成者: 本山, 三知代, 渡邊, 源哉, 佐々木, 啓介 メールアドレス: 所属:
URL	https://repository.naro.go.jp/records/2514

This work is licensed under a Creative Commons Attribution-NonCommercial-ShareAlike 3.0 International License.

Accepted Manuscript

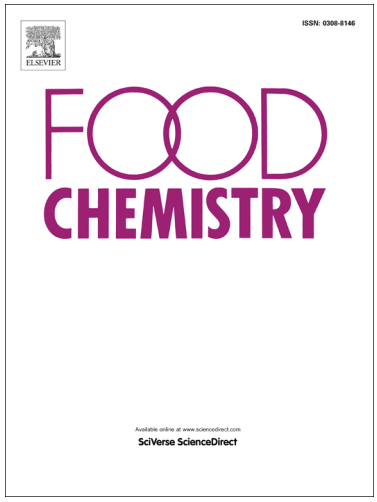

In situ characterization of acidic and thermal protein denaturation by infrared microspectroscopy

Michiyo Motoyama, Annie Vénien, Olivier Loison, Christophe Sandt, Genya Watanabe, Jason Sicard, Keisuke Sasaki, Thierry Astruc

PII: S0308-8146(17)31842-3
DOI: https://doi.org/10.1016/j.foodchem.2017.11.031
Reference: FOCH 22008

To appear in: *Food Chemistry*

Received Date: 11 July 2017
Revised Date: 8 November 2017
Accepted Date: 8 November 2017

Please cite this article as: Motoyama, M., Vénien, A., Loison, O., Sandt, C., Watanabe, G., Sicard, J., Sasaki, K., Astruc, T., *In situ* characterization of acidic and thermal protein denaturation by infrared microspectroscopy, *Food Chemistry* (2017), doi: https://doi.org/10.1016/j.foodchem.2017.11.031

This is a PDF file of an unedited manuscript that has been accepted for publication. As a service to our customers we are providing this early version of the manuscript. The manuscript will undergo copyediting, typesetting, and review of the resulting proof before it is published in its final form. Please note that during the production process errors may be discovered which could affect the content, and all legal disclaimers that apply to the journal pertain.

ACCEPTED MANUSCRIPT

Title

In situ characterization of acidic and thermal protein denaturation by infrared microspectroscopy

Authors

Michiyo Motoyama[1,2*], Annie Vénien[1], Olivier Loison[1], Christophe Sandt[3], Genya Watanabe[2], Jason Sicard[1], Keisuke Sasaki[2], Thierry Astruc[1†]

Affiliations

[1]UR370 Qualité des Produits Animaux, Institut National de la Recherche Agronomique (INRA), 63122 Saint-Genès-Champanelle, France

[2] Institute of Livestock and Grassland Science, National Agriculture and Food Research Organization (NARO), Tsukuba, 305-0901, Japan

[3] SMIS beamline, Synchrotron SOLEIL, Orme des merisiers, BP48, 91192 Gif-sur-Yvette, France

[†] Joint first author

Corresponding author telephone and fax

Tel and fax: +81 29 838 8690 (M. Motoyama)

Email addresses

[*]Michiyo Motoyama, mmichiyo@affrc.go.jp / michiyo.motoyama@inra.fr

Annie Vénien, annie.venien@inra.fr

Olivier Loison, olivier.loison@inra.fr

ACCEPTED MANUSCRIPT

Christophe Sandt, christophe.sandt@synchrotron-soleil.fr

Genya Watanabe, watanabeg080@affrc.go.jp

Jason Sicard, jason.sicard@inra.fr

Keisuke Sasaki, ksuk@affrc.go.jp

†Thierry Astruc, thierry.astruc@inra.fr

Abstract

Foods meet acid pH during gastric digestion after cooking. An *in situ* infrared microspectroscopy approach was developed to detect the effects of heat and acid treatments on protein structure separately. Infrared spectra were obtained from meat samples treated with heat and/or acid, and wavenumbers accounting independently for the treatments were extracted by principal component regression. Extreme-acid treatment ($pH_{initial}$ 2.0) was well predicted (0.5% error) by a simple ratio of as-observed spectral intensities at 1211 and 1396 cm^{-1}, reflecting a perturbation in the vibration of amino acid residues (phenylalanine, tyrosine and aspartic acid) by protein unfolding and protonation. Using the imaging mode of an IR microscope, meat protein acidification was evidenced with high spatial resolution. The heat effect was well discriminated from the acid effect by the ratio of as-observed intensities at 1666 and 1697 cm^{-1} (0.9% error), indicating content of aggregated β-sheets relative to α-helix structure.

Keywords

Infrared microscopy; meat; acidic pH; heat treatment; protein denaturation

ACCEPTED MANUSCRIPT

Main text

1. Introduction

Food proteins are exposed to heat and acid pH during processing, cooking and gastric digestion. Since digestibility, nutritive quality and allergenic behavior of food proteins are affected by pH and heat treatments (He, Simpson, Ngadi, & Ma, 2015; Kondjoyan, Daudin, & Sante-Lhoutellier, 2015; Lang, Kagiya, & Kitta, 2015; Sante-Lhoutellier, Astruc, Marinova, Greve, & Gatellier, 2008), the study of pH and thermal behavior of food proteins is important for determining and predicting the final quality of products.

Acid pH induces a number of changes in protein structure, such as protonation of amino acid residues, protein unfolding, and transformations in secondary and tertiary structures, that can be highlighted by vibrational spectroscopy. Protonation of residual carboxyl groups of acidic amino acids have served as a good vibrational spectroscopic probe for protein acidification (Litwińczuk, Ryu, Nafie, Lee, Kim, Jung, et al., 2014). Protein folding and packing states have been characterized by vibrational spectroscopy investigating backbone structure, strength of hydrogen bonding in secondary structure, or hydration state of side chains (Ashton & Blanch, 2010; Litwińczuk, et al., 2014). For such characterization, vibrational bands of side chain residues of aromatic amino acids, which are sensitive to microenvironmental change, and amide I and II bands, frequently provide information. Amide I and II vibrations accurately reflect the protein main-chain structure, and are commonly used for protein secondary structural analysis (Barth, 2007).

Heat-induced transition in protein structure has also been studied by analyzing vibrational spectra. Using the amide I band, IR spectroscopy reveals heat-induced α-helix unfolding and the formation of intermolecular β-sheet aggregation (Meersman, Smeller, & Heremans, 2002;

ACCEPTED MANUSCRIPT

Torrecillas, Corbalan-Garcia, & Gomez-Fernandez, 2004). Loss of α-helix and increase in β-sheet structure have been detected in meat, milk and legume-derived proteins (Herrero, Carmona, Lopez-Lopez, & Jimenez-Colmenero, 2008; Wu, Bertram, Böcker, Ofstad, & Kohler, 2007; Carbonaro, Maselli, Dore, & Nucara, 2008).

The combination of an infrared spectrometer and an infrared microscope allows measurements on small samples a few tens of microns in size, such as biological cells, either isolated or in tissues. Microspectroscopy has allowed protein structures of structured foods to be studied *in situ*. IR microscopy was used to detect tissue-dependent heat denaturation processes in meat connective tissue and muscle fibers (Kirschner, Ofstad, Skarpeid, Host, & Kohler, 2004). Our group used IR microscopy with a synchrotron radiation source to compare changes caused by heat denaturation in various type of muscle fiber and connective tissue proteins in meat, with a spatial resolution of 10 μm (Astruc, Peyrin, Venien, Labas, Abrantes, Dumas, et al., 2012).

The specific structural and environmental changes in protein caused by heat and acid treatments can be confounded in the infrared spectra of food, and it is not always easy to separate these effects. This is because (i) protein structural changes caused by the two treatments overlap, (ii) vibrational changes arising from protein structural changes affect other spatially or energetically proximate vibrations, and (iii) the spectral intensities of all the molecules in the sample are superimposed on detection.

The aim of the present study was to develop an IR microspectroscopic approach to discern the separate effects of acid and heat treatments on protein in meat *in situ*. Ideally, such a method should require minimum spectral preprocessing and obviate complex black-box analyses. We therefore opted for a method using peak intensity ratios. Spectral variables that account for these two treatments independently were extracted from IR spectra, allowing separate visualization of acid and heat effects with high spatial resolution.

ACCEPTED MANUSCRIPT

2. Materials and Methods

2.1. Samples

Beef was prepared as a sample material mainly composed of protein. Deltoid muscles (ca. 2.5 kg) from the right and left sides of a beef carcass (Charolaise breed, 90 months old) were prepared and vacuum-packed. Four days after slaughtering, one muscle was stored for 10 h under vacuum in a cold room (4 °C), while the contralateral muscle was vacuum-cooked at 85 °C for 10 h (an industrial practice for braising). After cooking, the muscle was cooled to 3 °C. Both raw and cooked muscles were then stored at 4 °C. Drip loss from the vacuum-packed beef was 1%, and the cooking loss was 33%.

On the same day as the cooking, the raw and cooked samples were cut into 1 cm × 1 cm × 2 cm pieces with the long axis parallel to the long axis of the muscle fibers. Each meat piece was placed in a 60 mL test tube and incubated with 50 mL of 0.9% NaCl solution, adjusted to pH 2.0, 3.5 or 5.0 ($pH_{initial}$) with aqueous HCl, and gently shaken for 2 h at 37 °C. Three sample test tubes were used for each pH condition (triplicates). After 2 h incubation, meat samples were immediately cryofixed in cooled isopentane (−160 °C) and stored at −80°C.

Final pH (pH_{final}) of the NaCl solution was measured using a glass electrode at the end of meat incubation, and is shown in Table 1. The pH increased after the incubation in all the treatments because of the buffering capacity of the meat (Puolanne, & Kivikari, 2000). The pH of meat is weakly acidic, and it is higher than that of the incubation solutions. The pH in the solution of $pH_{initial}$ = 3.5 increased remarkably because proton (H^+) consumption by protonation of amino acid residues of the meat protein was relatively larger than the H^+ amount that initially existed in the employed solution (Supplementary Material 1).

ACCEPTED MANUSCRIPT

The cryofixed samples were cryosectioned transversally to the muscle fibers (6 µm thickness) and thaw-mounted on BaF_2 windows compatible with IR spectroscopy. Serial sections were prepared for histological staining. The sections were vacuum-packed and stored at −20°C until spectroscopic measurement to avoid sample auto-oxidation.

2.2. IR microspectroscopy

2.2.1. IR spectral acquisition and pretreatment

FT-IR spectra of single muscle fibers were acquired with an IR microscope equipped with a mercury-cadmium-tellurium detector (Nicolet iN10, ThermoFisher) with a spectral resolution of 4 cm^{-1}. A spatial resolution of 20 µm × 20 µm was used, which was smaller than the muscle fiber dissection area. For each spectrum, 128 scans were accumulated and averaged. A background spectrum was obtained and automatically subtracted from every batch of spectral acquisitions. "As-observed spectra" in what follows refer to these background-subtracted spectra.

From each meat sample section, about 40 spectra were obtained from different single fibers located at the surface of the meat samples, assumed to undergo the direct effect of the acid bath (Supplementary Material 2). A total of 684 spectra (38 fibers × 3 acid treatments × 3 replicates × 2 heat treatments) were obtained.

2.2.2. IR chemical mapping of meat sections

In order to create chemical images of the sample sections, IR spectral maps of large areas were obtained by raster scanning the sample using a computer-controlled x-y stage with steps

ACCEPTED MANUSCRIPT

of 20 μm × 20 μm. Values obtained from spectral analysis were mapped onto the corresponding optical image to create the chemical images of acid and heat treatments.

2.3. Histological staining

Sections were stained with picro Sirius red, which shows the collagen of perimysium and endomysium in red and the muscle cells in yellow, while adipocytes are not stained and remain white (Flint & Pickering, 1984).

2.4. Statistical analysis

2.4.1. Data mining

Multivariate statistical analysis was used to explore the variance in the spectral data set (range 1900–800 cm^{-1}). Principal component analysis (PCA) and principal component regression (PCR) were performed using The Unscrambler software version 9.8 (CAMO Software AS). In order to exclude the effects of fluctuation in baseline due to light scattering and the effects of non-uniform sample section thickness, spectra were processed by extended multiplicative signal correction (EMSC) (Kohler, Kirschner, Oust, & Martens, 2005).

PCA and PCR were carried out on EMSC preprocessed mean-centered spectra with the non-linear iterative partial least squares (NIPALS) algorithm using random cross validation with 20 segments and weights of 1.0 for all the spectral variables. PCR was conducted, assigning the spectral data as independent variables and the existence or non-existence of each treatment as dummy two-valued dependent variables. Cross validation was performed to create a reliable PCR model with a significance value of 0.05. PCR factor loadings were used

ACCEPTED MANUSCRIPT

to select the spectral variables, which were closely correlated with the effect of acid or heat treatment. When a number of successive spectral variables showed high correlation, the variable that showed the least correlation with the other treatment was selected.

2.4.2. IR index calculation and performance evaluation

IR indices for detecting the acid and heat treatments were created using the following equation:

$$IR_{\text{treatment}} = \frac{I_{ij}}{I_{ik}}$$

where I_{ij} and I_{ik} are the intensities of as-observed spectrum i at wavenumber j and k respectively after the spectra were offset-corrected at 1800 cm^{-1} to eliminate light scattering effects.

To select the best performing IR indices, ratios of the selected spectral variables (2.4.1) were systematically computed, while the discriminatory power of the developed indices was assessed using the DISCRIM procedure of SAS (version 9.4, SAS Institute Inc., Cary, NC, USA). More specifically, Mahalanobis square distances from the means of index value of both groups with or without treatment with each data point was calculated, while prediction error was evaluated on the assumption that each data point was classified into the close group.

Differences between index values of treatment groups were tested by a Tukey-Kramer test at 5% significance using the GLM procedure of SAS. The $pH_{initial}$ and cooking state, and their first-order interaction were assigned as the variables of the statistical model. The normality of the index values of each sample group was validated beforehand by the Shapiro-Wilk test using the UNIVARIATE procedure of SAS, and the equality of variance and normality of the data was ensured by Box-Cox transformation using the TRANSREG procedure of SAS.

ACCEPTED MANUSCRIPT

3. Results and Discussion

3.1. Characteristics of IR spectra

Mean spectra of the muscle fibers from the incubated meat are shown in Fig. 1. Spectral variability originated from the transformation and protonation of protein caused by heat and acid treatments. In the amide I region (1700–1600 cm^{-1}), a higher band intensity at 1630 cm^{-1} relative to 1655 cm^{-1} was observed in both more acidic and cooked samples. In the vicinity of 1630 cm^{-1}, more than one band was reported to exist, and they originate from the aggregated β-sheet and solvated α-helix structures of protein (Barth, 2007; Gilmanshin, Williams, Callender, Woodruff & Dyer, 1997). In contrast, 1655-cm^{-1} band originates from the native α-helix structure (Barth, 2007; Böcker, et al., 2007). Aggregated β-sheet structure also gave a shoulder band at around 1695, which is a splitting band of the amide I mode. The band shape of amide II (1600–1500 cm^{-1}) also changed after the treatments, i.e., the highest peak around 1540 cm^{-1} and its shoulder peak around 1520 cm^{-1} became broader and the band feature gradually disappeared. Amide II is sensitive to protein main chain structure, and hardly affected by side chain vibrations similarly to amide I mode (Oberg, Ruysschaert, & Goormaghtigh, 2004; Barth, 2007). Changes were also observed in the 1400–1200 cm^{-1} region. In this region, there is an amide III protein-main chain mode, which is affected by protein side chain structures, together with other vibrational modes such as CH bending, and tyrosine and phenylalanine ring vibrations. Intensities at around 1400 and 1300 cm^{-1} decreased with both acid and heat treatments.

Food proteins generally undergo both heat and acid treatments during food production and digestion processes, and so both effects may be substantially superimposed in the spectra.

ACCEPTED MANUSCRIPT

In order to detect specific changes related to each treatment separately (acid effect or heat effect) and identify the protein structural changes involved, a multivariate analysis of the spectra obtained from meat proteins treated with acid and/or heat treatments was conducted.

The unsupervised PCA was performed first to investigate the spectral differences in the spectral data set. The score plot of principal components (PC 1 versus PC 2) displayed a distinct clustering according to the treatments (Fig. 2A top). PC 1 explained 58% of the total variance in the data set, and clearly separated the samples according to the treatment. The clusters were significantly more widespread in cooked samples, indicating a broader variation in their spectra than in those of raw samples, consistent with an earlier study (Kirschner et al., 2004). PC 2 explained 26% of the total variance, and clearly discerned the samples of $pH_{initial}$ 2.0 from those of $pH_{initial}$ 3.5 and 5.0. PC 2 did not separate the samples of $pH_{initial}$ 3.5 and 5.0. This is probably attributable to a small difference in their final pH (Table 1).

Loading vectors of the PCs are shown in the bottom panel of Fig. 2A. Loading vectors of the PC 1 were strongly positive at 1520, 1623, and 1697 cm^{-1}, corresponding to the amide II and amide I bands of the β-sheet structure (Barth, 2007; Pelton, & McLean, 2000). By contrast, loadings were strongly negative at 1654 and 1300 cm^{-1}, which are respectively amide I and III bands of the α-helix structure (Barth, 2007; Fu, Deoliveira, Trumble, Sarkar, & Singh, 1994). Loss of α-helix and increase in β-sheet have been reported as structural changes due to the heat effect (Meersman et al., 2002; Torrecillas et al., 2004). PC 1 accounts for these changes.

Loading vectors of the PC 2 were strongly positive at 1628, 1722 and 1215–1180 cm^{-1}; they are respectively assigned to β-sheet structure and/or solvated α-helix structures (Pelton, & McLean, 2000; Gilmanshin et al, 1997), to aspartic acid (Asp) side-chain C=O stretch mode in acidic pH (Venyaminov, & Kalnin, 1990; Litwińczuk, et al., 2014), and tentatively to aromatic ring mode of phenylalanine (Phe) and tyrosine (Tyr) side chains, which are known to

ACCEPTED MANUSCRIPT

form a core of hydrophobicity contributing to protein folding (Colthup, Daly, & Wilberley, 1990; Lord & Yu, 1970). By contrast, it was strongly negative at 1575, 1393 and 1685 cm^{-1}. 1575 and 1393 cm^{-1} are respectively assigned to antisymmetric and symmetric stretch modes of $–COO^-$ of non-protonated Asp side-chain (Venyaminov, & Kalnin, 1990; Colthup et al., 1990; Litwińczuk, et al., 2014). Intensity at 1575 cm^{-1} probably also comprised contributions of main-chain amide I and II bands. Absorption at 1685 cm^{-1} might be attributed to main-chain turn structure (Pelton and McLean, 2000). PC 2 probably detected acid-induced protonation of protein side chains, transformations in secondary structure and protein unfolding.

PCR was then performed to identify characteristic infrared absorption frequencies correlated with each treatment, and spectral variables able to discriminate between the two treatments. Since PCA had shown that only 2 PCs were sufficient to capture 84% of the total variance and discriminate between the acid and heat treatments, PC 1 and PC 2 were used in the PCR. Fig. 2B shows the correlation loading plot of the 2 PCs. These PCs are orthogonal to each other, not only in how they appear, but also in the mathematical sense, i.e. they each capture variance related to an independent (to the first order) source of variation. The correlation loading plot also identifies which of the independent variables (infrared absorption intensities) are closely correlated with the dependent variables (treatment).

It can be seen from Fig. 2B that the PCR model identified absorption intensity at 1211 and 1724 cm^{-1} as strongly correlated with the $pH_{initial}$ 2.0 treatment, intensities at 1396, 1585 and 1551 cm^{-1} as strongly anti-correlated with the $pH_{initial}$ 2.0 treatment, and loosely connected to the $pH_{initial}$ 5.0 and $pH_{initial}$ 3.5 treatments. Regarding heat treatment, intensities at 1524, 1608, 1434 and 1697 cm^{-1} were strongly correlated with the cooked status, and intensities at 1666–1643 and 1296 cm^{-1} were strongly correlated to the raw status. These

ACCEPTED MANUSCRIPT

spectral variables were selected for evaluation as possible IR spectroscopic indices for acid and heat treatments.

3.2. IR index for acidification effect

Spectral variables of 1211 cm^{-1} had the highest PC 2 correlation coefficient (0.92) with a weak correlation with PC 1 (0.05), and accounted accurately for the effect of extreme acid treatment ($pH_{initial}$ 2.0) independently of heat treatment (Fig. 2B). This band is probably due to a vibration of the aromatic ring of Phe and Tyr, more specifically 1,3,5-radial carbon in-phase stretch mode involving substituent bond (–CH_2–) stretching (Colthup et al., 1990; Lord & Yu, 1970). Side chains of Phe and Tyr have no charge, and are packed inside a protein molecule in a hydrophobic environment. When proteins are exposed to an extremely acidic environment, they unfold, and these side chains are exposed to the aqueous phase (Ashton & Blanch, 2010). This microenvironmental change probably perturbs the side-chain vibration and alters the spectral intensity at 1211 cm^{-1}.

On the other hand, the symmetric –COO^- stretch vibration of Asp side chain at 1396 cm^{-1} was anti-correlated with the $pH_{initial}$ 2.0 treatment (Fig. 2B). Asp composes 9% of meat protein (FAO, 1970) and exhibits this intensive infrared absorption (molar attenuation coefficient E_0 = 256 L mol^{-1} cm^{-1}, Venyaminov, & Kalnin, 1990). The pK_a value of this –COO^- group is 3.7–3.9, and the protonation decreased the band intensity.

Using spectral intensities at these wavenumbers, an IR spectroscopic index to detect acid effect independently of that of heat was defined:

$$IR_{\mathrm{acid}} = \frac{I_{1211}}{I_{1396}}$$

where I denotes the net absorbance intensity of the IR spectrum at the wavenumber identified by a subscript. Intensity at 1800 cm^{-1} was taken as the baseline level (zero), since there are no

ACCEPTED MANUSCRIPT

fundamental vibrations in the 2000–1800 cm^{-1} spectral region (Larkin, 2011), and no band was observed there (Fig. 1).

IR_{acid} values obtained from as-observed spectra of muscle fibers are plotted in Fig. 3A. The index values were well accounted for by the acid treatment ($p < 0.001$), and the heat treatment did not affect the values ($p = 0.85$). The value was significantly higher in $pH_{initial}$ 2.0 samples than in $pH_{initial}$ 3.5 and 5.0 samples in both raw and cooked treatments. The IR_{acid} ranged from 0.58 ± 0.04 (average ± s.d.) in $pH_{initial}$ 5.0 and 3.5 samples to 0.84 ± 0.06 in $pH_{initial}$ 2.0 samples. Discriminant analysis showed that the prediction error of this index between $pH_{initial}$ 2.0 and $pH_{initial}$ 3.5 and 5.0 groups was 0.5%. This simple index value discerned the extreme acid treatment remarkably well.

In addition to I_{1211}/I_{1396}, intensity ratios using other spectral variables that had high correlation with acid treatment (1724, 1585 and 1551, Fig. 2B) were systematically tested; however, they were inferior to I_{1211}/I_{1396} in discriminant power. The second most effective index was I_{1211}/I_{1585} with a prediction error of 1.2%.

Ashton and Blanch (2010) identified three distinct stages in protein conformational transition along an acidification scale (from pH 6.5 to 1.8), and reported that for the first two transition phases the conformational changes occurred predominantly in the backbone secondary structure, while in the final transition phase (~pH 3.6–1.8) changes occurred in both secondary structure and side chain residue. Since the absorptions at 1211 and 1396 cm^{-1} both originate significantly from side chains, the IR_{acid} index probably specifically detects the transition of the final phase.

Since the correlation coefficient with PC 2 of I_{1396} was greater than that of I_{1211} (−0.975 and 0.916, respectively), I_{1396} had a greater impact on the index discriminant power than I_{1211}. The IR_{acid} index may therefore be more sensitive to the Asp side-chain protonation at p*K*a 3.7–3.9 than to the protein unfolding reported to occur below pH 2.5 in myosin, the single

ACCEPTED MANUSCRIPT

most abundant protein in muscle (Kristinsson & Hultin, 2003). The IR_{acid} index probably discriminates high or low pH compared with 3.7–3.9. This pH value corresponds to the upper limit of pH for pepsin activity: above pH 3.9, pepsin activity decreases to about 5% of its optimal activity at pH 2 (Kondjoyan et al., 2015).

3.3. IR index for heat effect

In addition to the IR_{acid} index, we wanted to create an index that would account for heat treatment independently of acid treatment. Similarly to the process of IR_{acid} development, ratios of absorption intensities at the spectral wavenumbers that were closely correlated with heat treatment and independent of acid treatment (Fig. 2B) were systematically tested.

It was found that I_{1697}/I_{1666} discriminated cooked and raw samples well, with the smallest prediction error of 0.9%. The band at 1697 cm^{-1} originates from aggregated β-sheets formed by protein thermal aggregation (Böcker et al., 2007; Wu et al., 2007). Protein thermal aggregation forms intermolecular β-sheets and very strong hydrogen bonds. By contrast, the intensity at 1666 cm^{-1} has a considerable contribution from the amide I band of the α-helix structure. An increase in the value of this ratio therefore means an increase in aggregated β-sheets relative to α-helix structures, and this structural change has been reported as a predominant change in protein thermal denaturation probed by IR spectroscopy (Meersman et al., 2002; Torrecillas et al., 2004; Astruc et al., 2012; Kirschner et al., 2004). An IR spectroscopic index to detect heat effect was therefore defined as:

$$IR_{\mathrm{heat}} = \frac{I_{1697}}{I_{1666}}$$

The values of this index obtained from as-observed spectra of muscle fibers are shown in Fig. 3B. They were well accounted for by the heat treatment ($p < 0.001$) and ranged from

ACCEPTED MANUSCRIPT

0.30 ± 0.03 in raw samples to 0.45 ± 0.04 in cooked samples. This index discriminated samples according to their heat treatment.

Aggregated β-sheet structure shows a band splitting of amide I mode (Arrondo & Goni, 1999; Barth, 2007); 1697 cm^{-1} in the numerator of the index is one of the split bands, and another more intense band is at 1630 cm^{-1}. Kirschner et al. (2004) reported that the band observed at 1630 cm^{-1} changed its intensity when subjected to heat treatment. In the present study, however, absorption at 1632–1628 cm^{-1} was also affected by pH acidification (Fig. 2B), making it less well suited as a specific marker for heat denaturation. In the vicinity of 1630 cm^{-1}, more than one spectral component is observed (Surewicz, Mantsch & Chapman, 1993; Haris & Chapman, 1995). Several studies reported that a band reflected the solvation of α-helix structure (Gilmanshin et al., 1997; Murayama & Tomida, 2004; Ferrer, Bosch, Yantorno & Baran, 2008) and is assigned to the additional hydrogen bonding of the solvent accessible backbone CO groups of α-helix to water (Reisdorf & Krimm, 1996). Protein unfolding by pH acidification changes the solvate location on the protein surface, and it might increase the intensity at 1630 cm^{-1}. Meanwhile, the band at 1697 cm^{-1} was little affected by acid treatment because of its lower sensitivity to hydrogen bonding strength (Krimm & Bandekar, 1986; Barth, 2007).

Although the spectral variables at 1666 cm^{-1} showed the smallest effect of acid treatment among the variables corresponding to the amide I band of α-helix (1666–1643 cm^{-1}, Fig. 2B) and contributed to the smallest prediction error of the IR_{heat} index, the other variables (1662–1643 cm^{-1}) also gave small errors (e.g. I_{1697}/I_{1654}, 1.9%). On the other hand, when the intensity at 1296 cm^{-1} (amide II band of α-helix), which had a weaker correlation with acid treatment than 1666 cm^{-1} (Fig. 2B) was used, the prediction error was much larger (e.g. I_{1697}/I_{1296}, 13.5%). This was because of an insufficiently large difference in the index values between raw and cooked samples obtained by the simple equation, and the large

ACCEPTED MANUSCRIPT

spectral variance in cooked samples. Larger prediction errors were also given using other variables (1524, 1608 and 1434 cm^{-1}, Fig. 2B) for the same reason. The value of spectral intensity and its variance together with the correlation coefficient with the treatment were the important factors for index development with a small prediction error.

3.4. IR index mapping

Fig. 4 (top) presents micrographs of two large sections of meat that were both exposed to $pH_{initial}$ 2.0; one was left raw while the other was cooked. Negative control sections that were not exposed to any acid treatment are also shown (Fig. 4 bottom). Spectra of muscle fibers were recorded in three different regions on each large section. The IR_{acid} index (I_{1211}/I_{1396}) was computed for each spectrum, and is indicated on the corresponding muscle fiber (Fig. 4A). IR_{acid} showed, as expected, that acidity was high near the surface of the sample and low inside it in both the raw and the cooked meat with the $pH_{initial}$ 2.0 treatment. In the cooked sample however, some points estimated to have high acidity were observed inside the meat. Since a liquid-like substance was observed at the approximate gap space by optical microscopy, oils flowing from adipose tissue probably influenced the index value. Oils have a totally different spectral shape from that of protein, and generate high IR_{acid} values.

Histological and chemical mapping images of IR_{acid} of a meat tissue treated in extreme acid conditions ($pH_{initial}$ 2.0) are shown in Figs. 5A and 5B. Pixels with IR_{acid} values outside the range 0.50–0.93 were excluded from the picture, effectively removing outlier spectra and pixels corresponding to connective tissue, adipose tissue or gaps in the section. From the mapping image, it can be seen that that depth where the sample beef was estimated to have pH < 3.7–3.9 was 1.5 mm from the sample surface after 2 h incubation. This result was

ACCEPTED MANUSCRIPT

consistent with the value of proton diffusivity of $3.5 \cdot 10^{-11}$ m^2/s in beef (Lebert & Daudin, 2014, Supplementary Material 3).

IR_{heat} (I_{1697}/I_{1666}) values were also calculated for the spectra and gave accurate results (Fig. 4B). Its value was low in raw samples and high in cooked samples, indicating that the cooked meat proteins had more aggregated β-sheet structure than the raw sample, confirming the observations of Kirschner et al. (2004) and Astruc et al. (2012). In Fig. 5C, the protein part (muscle fibers) of the sample gave small IR_{heat} values, and indicated correctly that the sample was raw without being affected by the existing pH gradient (shown in Fig. 5B). In contrast to the IR_{acid} index however, pixels related to fats and gaps did not in general give an outlier value. If fats, gap or any other components that are not protein occur in a sample, and if it is not possible to identify them by optical microscopy, the infrared spectra should be checked beforehand to identify the nature of the tissue, and determine whether it is truly protein.

3.5. Notes for application

The IR method developed is probably applicable directly for proteins that have amino-acid compositions somewhat similar to that of muscle fiber. However, if amino acid composition differs, and therefore the protein secondary structures, then the value of IR indices may vary. Collagen, for example, is known for its specific amino acid composition: its Phe and Tyr percentage is almost double of that of muscle fiber (Lin, & Liu, 2006). Its spectrum may therefore exhibit higher intensities at 1211 cm^{-1}; consequently, connective tissue generated the outlier IR_{acid} value (higher side) in the present study as already described. The IR_{heat} value can also vary, since quantity of secondary structures and denaturation temperature vary among proteins (Carbonaro et al., 2008; Oberg et al., 2004). In meat for

ACCEPTED MANUSCRIPT

example, decrease in α-helical structures by cooking was reported to be less pronounced in the connective tissue (mainly collagen) than in the muscle fibers (Kirschner et al., 2004, Astruc et al., 2012). Application of the IR indices for tissues other than muscle fibers should thus be a confirmation step to ensure accuracy.

Since obtaining a series of spectra to make a chemical map is time-consuming, a single spectrum obtained from a target sample point may be the most useful application of the IR indices. As already described, if there is material other than protein, the value of the indices can be affected. Obtaining several spectra from the same area may therefore be necessary, or a quality test on spectra to check whether they contain spectral components other than those of protein may be useful.

In addition to the above notes, other factors that may affect the index values have been reported. IR spectra of protein can be altered by pH readjustment to neutrality (Kristinsson & Hultin, 2003), ionic strength (Böcker, et al., 2007; Herrero, et al., 2008; Kukic, O'Meara, Hewage, & Nielsen, 2013), and by the sample condition of fresh or frozen-thawed (AlJowder, Kemsley, & Wilson, 1997). They affect the environment and protein structure, and this may change spectral intensities at wavenumbers of interest, and affect the index value. Attention should also be paid to the spectral measurement condition (transmission or reflection), IR frequency can be shifted by the conditions (Litwińczuk, et al., 2014). Care should also be taken to obtain spectra with intensities in the Amide I band between 0.3 and 1.2 absorbance units to stay in the linear range: spectra above and below these limits may present small distortions in the ratios between peaks.

4. Conclusion

ACCEPTED MANUSCRIPT

IR spectroscopy was used to monitor the structural changes of muscle fiber proteins in meat samples subjected to acidification and/or cooking *in situ*. The present study offers potential IR indices that allow the separate detection of acid and heat treatments. Simple spectral intensity ratios at certain wavenumbers of as-observed IR spectrum were validated.

Generally, proteins are digested after being subjected to acid and heat, and both treatments affect protein digestion by the digestive enzymes. Activity of enzymes depends on pH, and heat denaturation/aggregation of protein modifies the digestion rate of protein on a case-by-case basis (Kondjoyan et al. 2015, Lang et al. 2015, Bax et al. 2012). In meat, a relation between heat aggregation of myofibrillar proteins and the decrease in digestion rate by pepsin was reported (Sante-Lhoutellier et al. 2008). Digestibility affects not only bioavailability and nutritive value of the protein but also causes allergenic behavior, which results from the proteins which are not well digested. The *in situ* separate imaging of acid and heat effects of food matrix using IR indices can provide a realistic and comprehensive understanding of the bioavailability of food proteins.

To the best of our knowledge there is no simpler method to measure pH with high spatial resolution, and this IR method can be further refined in this respect. The IR_{acid} index showed whether a spectral acquisition point had a pH lower than 3.7–3.9 or not. It enabled us to easily tell whether the gastric digestive enzyme pepsin could be active there, with high spatial resolution of the order of 10 μm.

It would be of interest to increase resolution of pH or to expand this index to cover wider range of pH. It enabled us to visualize gradual pH change. Neutral or alkali pH could also be detected, protein structural changes in these pH ranges having been reported (Chehin, Iloro, Marcos, Villar, Shnyrov, & Arrondo, 1999). In the future, various forms of the IR spectroscopic index developed should be available as methods to visualize pH of foods *in situ* with high spatial resolution, independently of cooking state.

ACCEPTED MANUSCRIPT

Acknowledgments

The authors thank the Synchrotron SOLEIL SMIS beamline (Project Number 20150009) for technical assistance, and Charal for the sample meats. MM received the support of the EU in the framework of the Marie-Curie FP7 COFUND People Programme, through the award of an AgreenSkills fellowship (under grant agreement No. 267196).

Conflict of interest

Authors declare no conflict of interest.

References

AlJowder, O., Kemsley, E. K., & Wilson, R. H. (1997). Mid-infrared spectroscopy and authenticity problems in selected meats: A feasibility study. *Food Chemistry, 59*(2), 195-201.

Arrondo, J. L. R., & Goni, F. M. (1999). Structure and dynamics of membrane proteins as studied by infrared spectroscopy. *Progress in Biophysics & Molecular Biology, 72*(4), 367-405.

Ashton, L., & Blanch, E. W. (2010). pH-induced conformational transitions in alpha-lactalbumin investigated with two-dimensional Raman correlation variance plots and moving windows. *Journal of Molecular Structure, 974*(1-3), 132-138.

Astruc, T., Peyrin, F., Venien, A., Labas, R., Abrantes, M., Dumas, P., & Jamme, F. (2012). In situ thermal denaturation of myofibre sub-type proteins studied by immunohistofluorescence and synchrotron radiation FT-IR microspectroscopy. *Food Chemistry, 134*(2), 1044-1051.

ACCEPTED MANUSCRIPT

Barth, A. (2007). Infrared spectroscopy of proteins. *Biochimica Et Biophysica Acta-Bioenergetics, 1767*(9), 1073-1101.

Bax, M.-L., Aubry, L., Ferreira, C., Daudin, J.-D., Gatellier, P., Remond, D., & Sante-Lhoutellier, V. (2012). Cooking Temperature Is a Key Determinant of in Vitro Meat Protein Digestion Rate: Investigation of Underlying Mechanisms. *Journal of Agricultural and Food Chemistry, 60*(10), 2569-2576.

Böcker, U., Ofstad, R., Wu, Z. Y., Bertram, H. C., Sockalingum, G. D., Manfait, M., Egelandsdal, B., & Kohler, A. (2007). Revealing covariance structures in Fourier transform infrared and Raman microspectroscopy spectra: A study on pork muscle fiber tissue subjected to different processing parameters. *Applied Spectroscopy, 61*(10), 1032-1039.

Carbonaro, M., Maselli, P., Dore, P., & Nucara, A. (2008). Application of Fourier transform infrared spectroscopy to legume seed flour analysis. *Food Chemistry, 108*(1), 361-368.

Chehin, R., Iloro, I., Marcos, M. J., Villar, E., Shnyrov, V. L., & Arrondo, J. L. R. (1999). Thermal and pH-induced conformational changes of a β-sheet protein monitored by infrared spectroscopy. *Biochemistry, 38*(5), 1525-1530.

Colthup, N. B., Daly, L. H., & Wilberley, S. E. (1990). *Introduction to infrared and Raman spectroscopy* (Third ed.). Amsterdam: Academic press, Elsevier.

Ferrer, E. G., Bosch, A., Yantorno, O., & Baran, E. J. (2008). A spectroscopy approach for the study of the interactions of bioactive vanadium species with bovine serum albumin. *Bioorganic & Medicinal Chemistry, 16*(7), 3878-3886.

FAO (1970). Amino-acid content of foods and biological data on proteins. http://www.fao.org/docrep/005/AC854T/AC854T00.htm

Flint, F. O., & Pickering, K. (1984). Demonstration of collagen in meat-products by an improved picro-syrius red polarization method. *Analyst, 109*(11), 1505-1508.

ACCEPTED MANUSCRIPT

Fu, F. N., Deoliveira, D. B., Trumble, W. R., Sarkar, H. K., & Singh, B. R. (1994). Secondary structure estimation of proteins using the amide-III region of Fourier-transform infrared-spectroscopy—Application to analyze calcium binding-induced structural-changes in calsequestrin *Applied Spectroscopy, 48*(11), 1432-1441.

Gilmanshin, R., Williams, S., Callender, R. H., Woodruff, W. H., & Dyer, R. B. (1997). Fast events in protein folding: Relaxation dynamics of secondary and tertiary structure in native apomyoglobin. *Proceedings of the National Academy of Sciences of the United States of America*, *94*(8), 3709-3713.

Haris, P. I., & Chapman, D. (1995). The conformational analysis of peptides using Fourier transform IR spectroscopy. *Biopolymers*, *37*(4), 251-263.

He, S. D., Simpson, B. K., Ngadi, M. O., & Ma, Y. (2015). In vitro studies of the digestibility of lectin from black turtle bean (Phaseolus vulgaris). *Food Chemistry*, *173*, 397-404.

Herrero, A. M., Carmona, P., Lopez-Lopez, I., & Jimenez-Colmenero, F. (2008). Raman spectroscopic evaluation of meat batter structural changes induced by thermal treatment and salt addition. *Journal of Agricultural and Food Chemistry, 56*(16), 7119-7124.

Kirschner, C., Ofstad, R., Skarpeid, H. J., Host, V., & Kohler, A. (2004). Monitoring of denaturation processes in aged beef loin by Fourier transform infrared microspectroscopy. *Journal of Agricultural and Food Chemistry, 52*(12), 3920-3929.

Kohler, A., Kirschner, C., Oust, A., & Martens, H. (2005). Extended multiplicative signal correction as a tool for separation and characterization of physical and chemical information in Fourier transform infrared microscopy images of cryo-sections of beef loin. *Applied Spectroscopy*, *59*(6), 707-716.

ACCEPTED MANUSCRIPT

Kondjoyan, A., Daudin, J. D., & Sante-Lhoutellier, V. (2015). Modelling of pepsin digestibility of myofibrillar proteins and of variations due to heating. *Food Chemistry, 172*, 265-271.

Krimm, S., & Bandekar, J. (1986). Vibrational spectroscopy and conformation of peptides, polypeptides, and proteins. *Advances in Protein Chemistry, 38*, 181-364.

Kristinsson, H. G., & Hultin, H. O. (2003). Changes in conformation and subunit assembly of cod myosin at low and high pH and after subsequent refolding. *Journal of Agricultural and Food Chemistry, 51*(24), 7187-7196.

Kukic, P., O'Meara, F., Hewage, C., & Nielsen, J. E. (2013). Coupled effect of salt and pH on proteins probed with NMR spectroscopy. *Chemical Physics Letters, 579*, 114-121.

Lang, G. H., Kagiya, Y., & Kitta, K. (2015). Multiplex comparison of the digestibility of allergenic and non-allergenic proteins in rice grains by in vitro digestion. *Food Chemistry, 168*, 606-614.

Larkin, P. J. (2011). *Infrared and Raman spectroscopy: Principles and spectral interpretation*. Oxford: Elsevier.

Lebert, A., & Daudin, J. D. (2014). Modelling the distribution of a(w), pH and ions in marinated beef meat. *Meat Science, 97*(3), 347-357.

Lin, Y. K., & Liu, D. C. (2006). Comparison of physical-chemical properties of type I collagen from different species. *Food Chemistry, 99*(2), 244-251.

Litwińczuk, A., Ryu, S. R., Nafie, L. A., Lee, J. W., Kim, H. I., Jung, Y. M., & Czarnik-Matusewicz, B. (2014). The transition from the native to the acid-state characterized by multi-spectroscopy approach: Study for the holo-form of bovine alpha-lactalbumin. *Biochimica Et Biophysica Acta-Proteins and Proteomics, 1844*(3), 593-606.

ACCEPTED MANUSCRIPT

Lord, R. C., & Yu, N. T. (1970). Laser-excited Raman spectroscopy of biomolecules. 1. Native lysozyme and its constituent amino acids. *Journal of Molecular Biology, 50*(2), 509-524.

Meersman, F., Smeller, L., & Heremans, K. (2002). Comparative Fourier transform infrared spectroscopy study of cold-, pressure-, and heat-induced unfolding and aggregation of myoglobin. *Biophysical Journal, 82*(5), 2635-2644.

Murayama, K., & Tomida, M. (2004). Heat-induced secondary structure and conformation change of bovine serum albumin investigated by Fourier transform infrared spectroscopy. *Biochemistry, 43*(36), 11526-11532.

Oberg, K. A., Ruysschaert, J. M., & Goormaghtigh, E. (2004). The optimization of protein secondary structure determination with infrared and circular dichroism spectra. *European Journal of Biochemistry, 271*(14), 2937-2948.

Pelton, J. T., & McLean, L. R. (2000). Spectroscopic methods for analysis of protein secondary structure. *Analytical Biochemistry, 277*(2), 167-176.

Puolanne, E., & Kivikari, R. (2000). Determination of the buffering capacity of postrigor meat. *Meat Science, 56*(1), 7-13.

Reisdorf, W. C., & Krimm, S. (1996). Infrared amide I' band of the coiled coil. *Biochemistry, 35*(5), 1383-1386.

Sante-Lhoutellier, V., Astruc, T., Marinova, P., Greve, E., & Gatellier, P. (2008). Effect of meat cooking on physicochemical state and in vitro digestibility of myofibrillar proteins. *Journal of Agricultural and Food Chemistry, 56*(4), 1488-1494.

Surewicz, W. K., Mantsch, H. H., & Chapman, D. (1993). Determination of protein secondary structure by Fourier transform infrared spectroscopy: A critical assessment. *Biochemistry, 32*(2), 389-394.

ACCEPTED MANUSCRIPT

Torrecillas, A., Corbalan-Garcia, S., & Gomez-Fernandez, J. C. (2004). An infrared spectroscopic study of the secondary structure of protein kinase C alpha and its thermal denaturation. *Biochemistry, 43*(8), 2332-2344.

Venyaminov, S. Y., & Kalnin, N. N. (1990). Quantitative IR spectrophotometry of peptide compounds in water (H_2O) solutions. 1. Spectral parameters of amino-acid residue absorption-bands. *Biopolymers, 30*(13-14), 1243-1257.

Wu, Z., Bertram, H. C., Böcker, U., Ofstad, R., & Kohler, A. (2007). Myowater dynamics and protein secondary structural changes as affected by heating rate in three pork qualities: A combined FT-IR microspectroscopic and H-1 NMR relaxometry study. *Journal of Agricultural and Food Chemistry, 55*(10), 3990-3997.

Figure captions

Fig. 1. Average IR spectra of muscle fibers of the meat after each treatment.

Fig. 2. Results of multivariate analysis of the spectral data (1900–800 cm^{-1}) of all the 684 muscle fiber samples in relation to the acid and heat treatments. (A) Score plots of PCA and loading vectors of PCs obtained. The variance explained by PC 1 and PC 2 were 58% and 26%, respectively. (B) Correlation loading plot (PC 1 versus PC 2) of PCR analysis. The inner and outer ellipses refer to 50% and 100% explained variance, respectively. Numeric characters indicate the spectral variables at corresponding wavenumbers.

Fig. 3. Box plots of the IR index values obtained from 684 as-observed spectra, showing median, 25 and 75 percentiles and minimum and maximum points. Outlier (×) is data whose

ACCEPTED MANUSCRIPT

index value was outside ±2σ. (A) IR_{acid}. (B) IR_{heat}. Data with different superscripts are significantly different ($p < 0.05$).

Fig. 4. Optical micrographs of sections and point maps of IR indices. "∗" corresponds to each point of spectral acquisition. Three fields of view of the samples on a BaF_2 window are overlaid onto the corresponding histological image of a stained section. Muscle fibers were stained yellow-orange, connective tissues red, and fats and gaps remained white. Top: Meat samples after 2 h incubation at $pH_{initial}$ 2.0. Bottom: Negative control sections without pH treatment. (A) IR_{acid}, (B) IR_{heat}.

Fig. 5. Optical microscopic view and IR chemical mapping images. (A) Optical view of a section of raw meat incubated in the solution of $pH_{initial}$ 2.0 (pH_{final} = 2.3). Top: Histologically stained section. Muscle fibers were stained yellow, connective tissues red, fats and gaps remained white. Lower: Optical view of the samples on BaF_2 window. (B) Mapping image of IR_{acid} index (top). Pixels colored black correspond to outliers. The merged image (bottom). (C) Mapping image of IR_{heat} index (top) and the merged image (bottom).

ACCEPTED MANUSCRIPT

ACCEPTED MANUSCRIPT

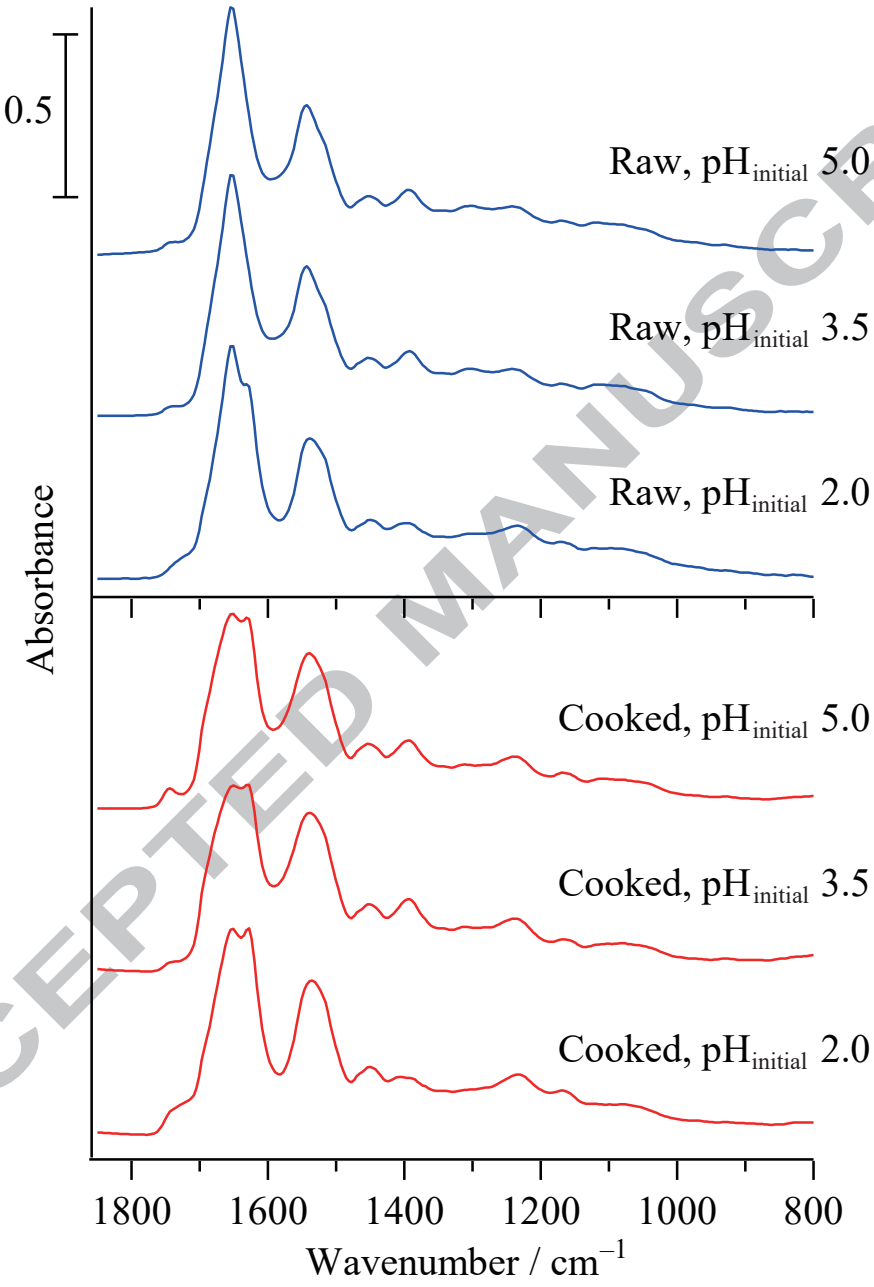

Fig. 1 (Motoyama et al.)

ACCEPTED MANUSCRIPT

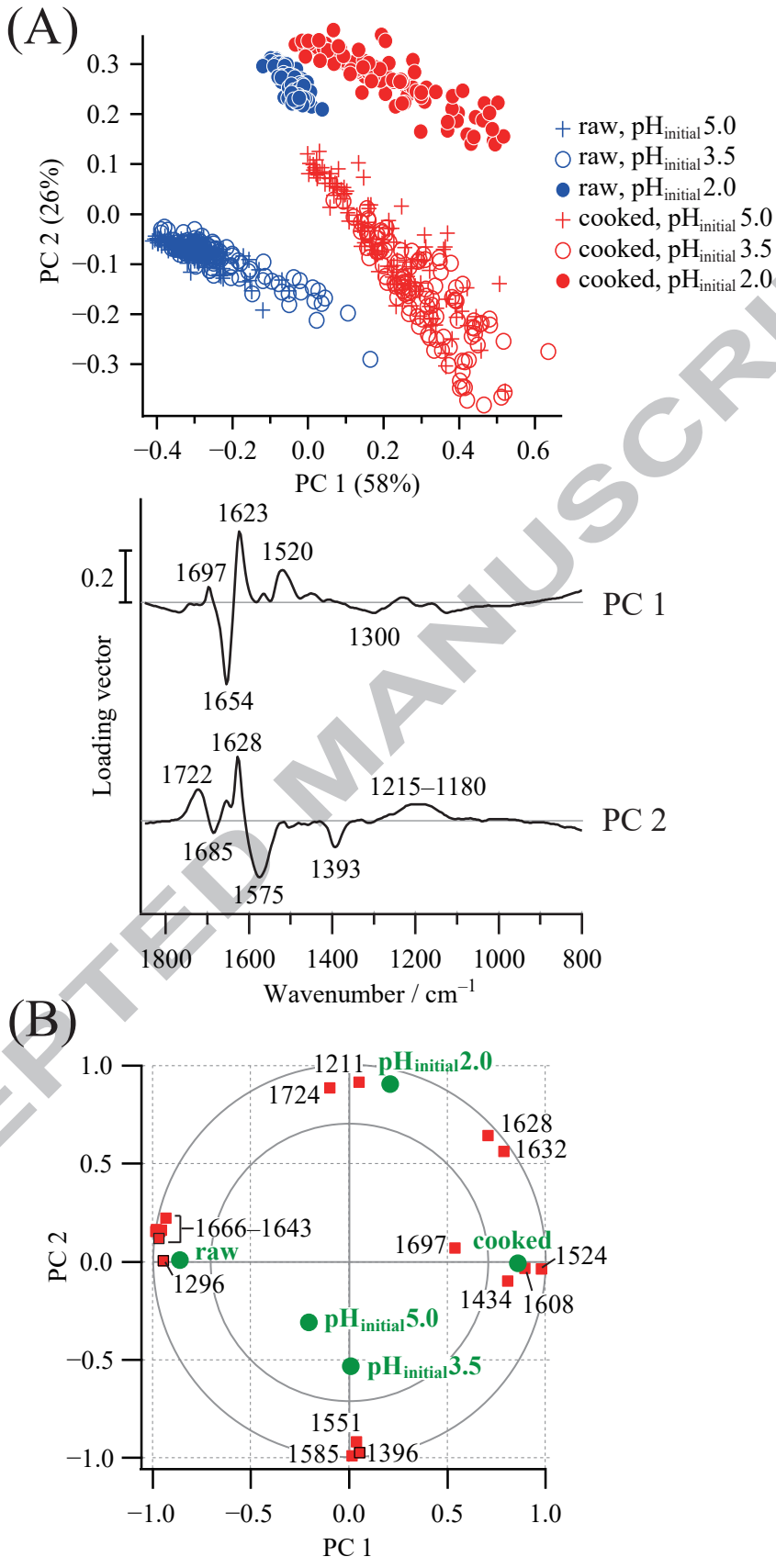

Fig. 2 (Motoyama et al.)

ACCEPTED MANUSCRIPT

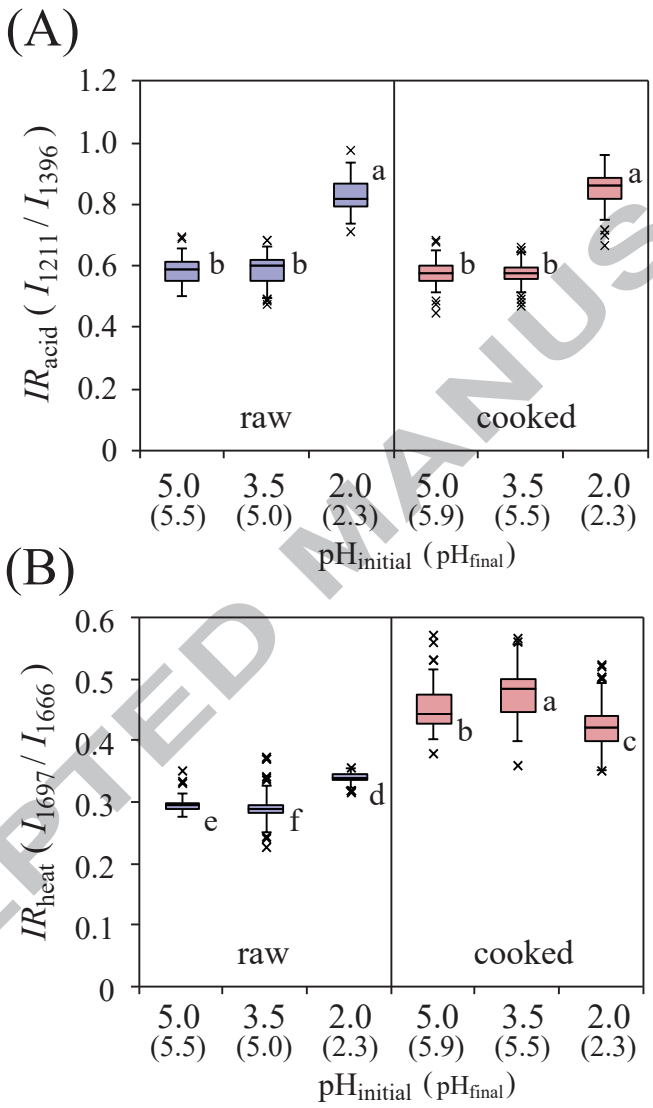

Fig. 3 (Motoyama et al.)

ACCEPTED MANUSCRIPT

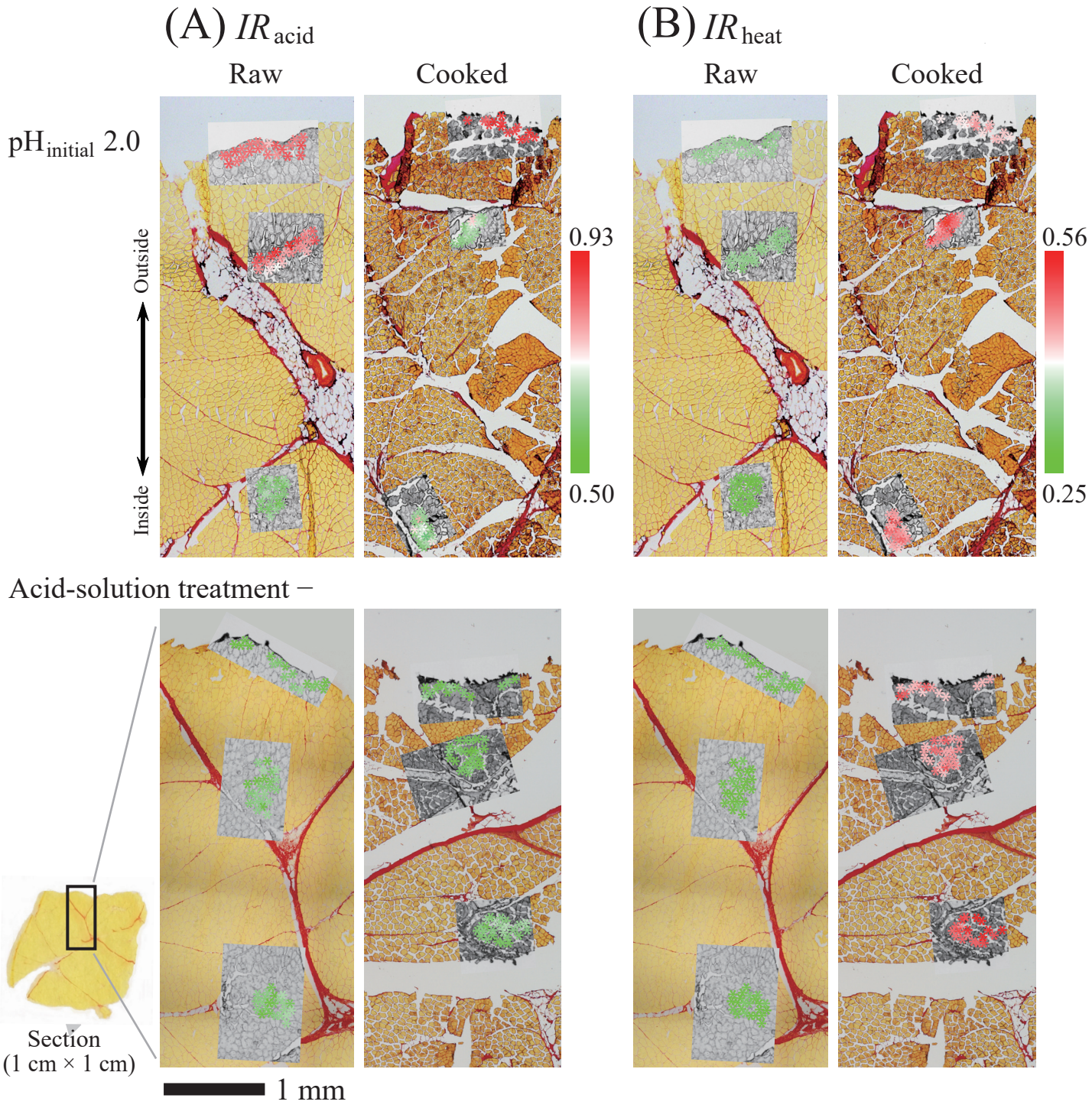

Fig. 4 (Motoyama et al.)

Print in color

ACCEPTED MANUSCRIPT

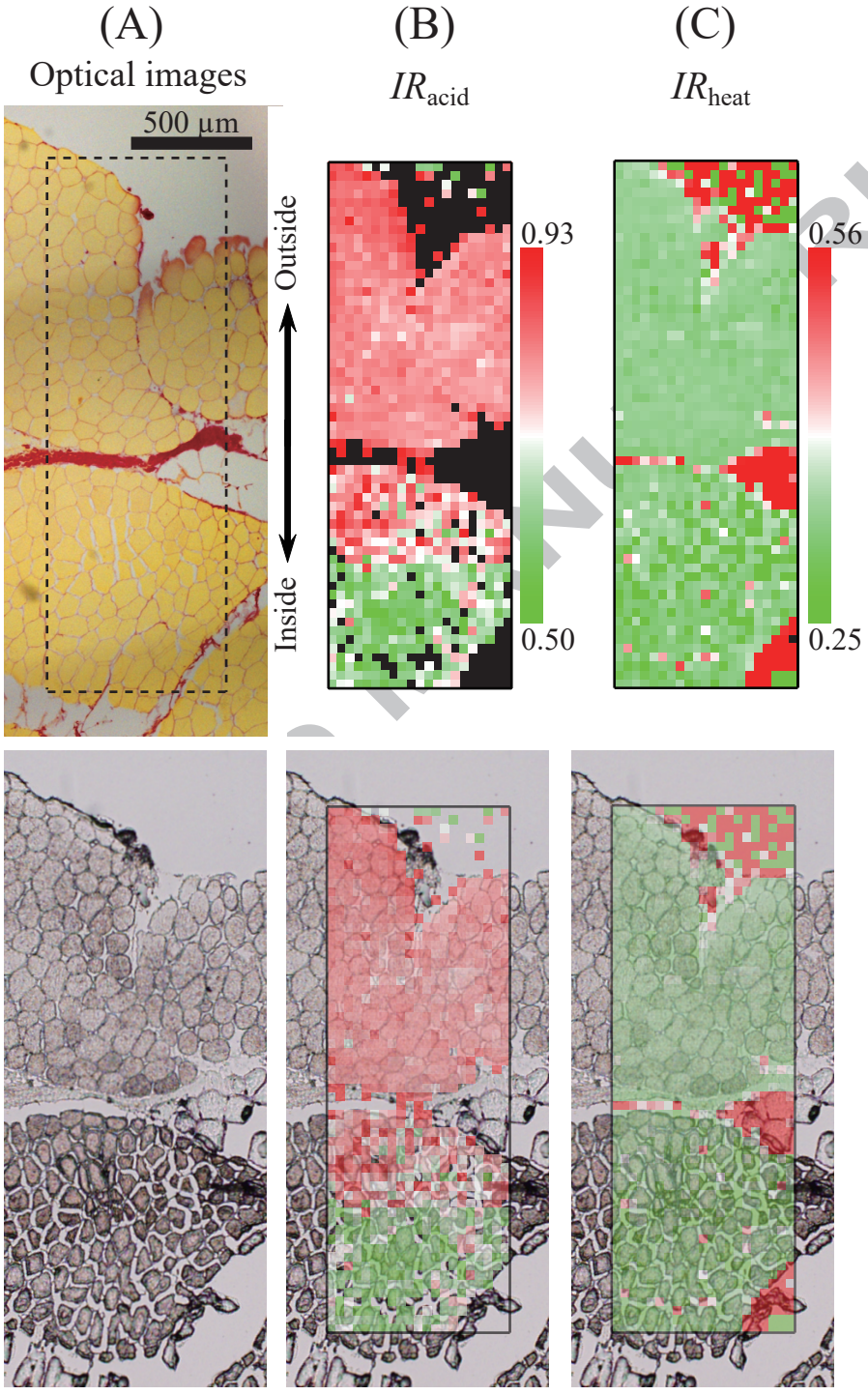

Fig. 5 (Motoyama et al.)

Print in color

ACCEPTED MANUSCRIPT

Table 1. Final pH value (average ± s.d.) of the incubation solutions of meat samples after 2 h incubation. Values with different superscripts are significantly different ($p < 0.001$).

$pH_{initial}$	pH_{final}	
	raw meat bath	cooked meat bath
5.0	5.5 ± 0.03^{b}	5.9 ± 0.01^{a}
3.5	5.0 ± 0.01^{c}	5.5 ± 0.06^{b}
2.0	2.3 ± 0.04^{d}	2.2 ± 0.02^{e}

ACCEPTED MANUSCRIPT

ACCEPTED MANUSCRIPT

Highlights

- Acid and heat effects on meat proteins were detected by IR microspectroscopy
- 1211/1396 cm^{-1} band ratio discerned acid effect independently of heat effect
- 1697/1666 cm^{-1} band ratio discerned heat effect independently of acid effect
- Acid pH can be detected with 10 μm resolution in meat sections by IR microscopy

ACCEPTED MANUSCRIPT